

Main characteristics and genesis of the Vale de Pães skarn (Cuba-Vidigueira, Ossa Morena Zone, Portugal)

Principales características y génesis del skarn de Vale de Pães (Cuba-Vidigueira, Ossa Morena Zone, Portugal)

R. Salgueiro¹, C. Inverno², A. Mateus³

ABSTRACT

The Vale de Pães (Cuba-Vidigueira) mineralisation is composed of magnetite ± sulphides and hosted in a Pre-Variscan metamorphic sequence intruded by igneous rocks belonging to the Beja Igneous Complex. Its mineral and chemical features are compatible with a zoned Fe-skarn: Mg-rich ($Fo + Di_{90}$, oxidised) and Ca-rich ($Grs + Di_{81-39}$, oxidised or relatively reduced). In the Fe-Mg skarn, magnetite deposition occurred along with the anhydrous mineral assemblage at ≈ 600 °C; sulphides precipitated from the retrograde stage onset (≤ 550 °C) and during the hydrated and carbonate phases formation period (< 420 °C). In the Fe-Ca skarn, magnetite precipitated during the retrograde stage (< 550 °C) together with the hydrated mineral association, and was followed by sulphides at ≈ 400 °C. The mineralising process involved moderate-high salinity fluids and was controlled by variations in redox potential and pH.

Key words: Magnetite-sulphide mineralisation, Fe(Mg/Ca) Skarn, Chemical zoning, Ossa Morena Zone.

RESUMEN

La mineralización del Vale de Pães (Cuba-Vidigueira), compuesta de magnetita ± sulfuros, se produce dentro de una secuencia metamórfica ante-Varisca intruida por el Complejo Ígneo de Beja (*Beja Igneous Complex*). Sus características químicas y mineralógicas son consistentes con un skarn de Fe zonificado: rico en Mg ($Fo + Di_{90}$, oxidado) y rico en Ca ($Grs + Di_{81-39}$, oxidado o relativamente reducido). En el skarn de Fe-Mg, la deposición de magnetita acompaña a la paragénesis mineral anhidra (≈ 600 °C); la precipitación de sulfuros se produce desde el comienzo de la etapa retrógrada (≤ 550 °C) y continuó durante la formación de fases hidratadas y carbonatadas (< 420 °C). En el skarn de Fe-Ca, la magnetita se genera en la fase de retroceso (< 550 °C), en relación con la asociación de minerales hidratados, seguido de sulfuro (≈ 400 °C). El proceso de mineralización de los fluidos de salinidad moderada-alta era controlado por los cambios en el potencial redox y el pH.

Palabras clave: mineralización de magnetita-sulfuros, Skarn de Fe(Mg/Ca), Zonificación química, Zona de Ossa Morena.

Introduction

The Vale de Pães (Cuba-Vidigueira) mineralisation is part of a set of small ore deposits included in the Magnetite-Zinc Belt of the Ossa-Morena Zone (e.g., Carvalho, 1976, Oliveira 1986). It was recognized during exploration surveys carried out by the

Serviço de Fomento Mineiro (SFM) since 1958. They included geological mapping (1:25000 scale), magnetometry and gravimetry surveys, and 25 drill-holes designed to intersect possible mineralised bodies suggested by magnetic anomalies. The hidden Vale de Pães deposit extends in depth up to 180 m and contains ≈ 9 Mt with average grades of

¹ Unidade de Investigação de Recursos Minerais e Geofísica, LNEG, Alfragide, Portugal. CeGUL e CREMINER-ISR LA Faculdade de Ciências da Universidade de Lisboa, Portugal. Email: rute.salgueiro@ineti.pt

² Unidade de Investigação de Recursos Minerais e Geofísica, LNEG, Alfragide, Portugal. CREMINER-ISR LA Faculdade de Ciências da Universidade de Lisboa, Portugal. Email: carlos.inverno@ineti.pt

³ Departamento de Geologia e CeGUL, Faculdade de Ciências da Universidade de Lisboa, Portugal. Email: amateus@fc.ul.pt

42 wt% Fe, 19 wt% SiO₂ and 0.6-5.2 wt% S (Carvalho, 1976, Oliveira 1986, Carvalho & Oliveira, 1992). Comprehensive examination of samples collected in one of the drill-holes performed in this area (SD42) allowed to recognise for the first time features that are crucial to the characterisation of these iron ores. The observed mineral assemblages, typical of skarn type deposits, include several calc-silicate minerals, magnetite and sulphides; this deposit typology is likewise compatible with the geological framework in which the Vale de Pães mineralisation developed. The present work intends to report and discuss these data, characterising the mineralised domains and the processes involved in the genesis of the Vale de Pães ore-forming system.

Sampling and analytical procedures

Representative samples were selected from the SD42 drill-hole core after comprehensive logging. Rock samples were analysed for major elements (Si, Ti, Al, Fe, Mg, Mn, Ca, Na, K, P) and some trace elements (Ba, Rb, S, Sr, Nb, Zr, Y, Sn) by X-ray-fluorescence spectrometry (XRF) performed at the ex-Instituto Geológico e Mineiro (IGM) Laboratory (Portugal); they were also analysed for Au by atomic absorption (AA) and for Cd and B by Coupled Plasma-Atomic Emission Spectrometry (DCP-AES) in the same laboratory; the estimated precision analytical errors were usually < 5-10% for major and trace elements. Complementary analyses were obtained at the Activation Laboratories Ltd (Canada) using the research grade package for Au + 48 elements that combines Inductively Coupled Plasma Optical Emission Spectrometry (ICP-OES; including Ni, V, Cu, Pb, Zn, Bi, Mo, Be, Ag) and Instrumental Neutron Activation Analyses (INAA; including La, Ce, Nd, Sm, Eu, Tb, Yb, Lu Cs, U, Th, Ta, Hf, Cr, Co Sc, W, Br, Ir, Au, Hg, As, Se, Sb); in terms of precision, the estimated analytical errors range from 5-10% on the measured content.

Electron microprobe analyses of pyroxene and olivine were made with a JEOL JXA 733-CG routinely operated with an acceleration potential of 15 kV and a beam current of 25 nA; the different mineral elements were analysed for 20s each; the analytical quality was controlled through measuring of natural and synthetic mineral standards before, during and after each work period; the analytical errors were less than 2% for the analysed elements.

Geological setting

In the Vale de Pães area, different igneous rocks (gabbros, diorites, granites and porphyries) belonging to the Beja Igneous Complex (BIC) intrude a pre-Variscan metamorphic suite containing marbles, amphibolic gneisses, chlorite-rich schists, amphibolites and metavolcanic (quartz-feldspar) rocks (Fig. 1A); contact domains between the two rock-suites are traced by undifferentiated hornfels and amphibolites (e.g., Piçarra *et al.*, 1992). The SD42 drill-hole is located in a contact domain and the recovered drill-hole core reveals a sequence of (volcanic, subvolcanic or intrusive) rocks that were metamorphosed in greenschist to amphibolite facies conditions (Salgueiro, *in prep*). Meta-felsic intercalations are present from 26 to 166.5 m depth, the thickest horizon occurring between 160 and 166.5 m (Fig. 1B). BIC intrusive rocks form different kinds of veins, veinlets and pseudo-intercalations, the main one identified between 185 and 192.04 m depth; quartz-monzonite (21.58-22.70 and 67.80-69.50 m) and granite (54.21-56.00 m) mineral assemblages appear to dominate in these BIC rocks (Fig. 1B). It is also noteworthy the presence of a meta-dolostone horizon between 178 and 185 m depth.

Mineralised domains

Characterisation of representative samples of the SD42 core allowed to distinguish several intervals of disseminated mineralisation with metric thickness, scattered between 86 and 105 m depth; these intervals include magnetite (*Mgt*) and sulphide-rich (centimetric) bands/levels. Between 105 and 157 m depth, five intervals of massive *Mgt* (\pm sulphides) mineralisation with metric thickness occur (106-109 m, 123-128 m, 135-138 m, 142-144 m and 153-157 m), forming intercalations with metamorphic and intrusive rocks (Fig. 1B). Considering the chemical features of the calc-silicate mineral assemblages accompanying the ore-forming phases (presented below) and according to the criteria reported by several authors (e.g., Purto *et al.*, 1989, Einaudi *et al.*, 1981), representative specimens of disseminated mineralisation are alike of Fe-Ca skarns (e.g., SD42/92, SD42/94, SD42/95 and SD42/98), while those representative of massive mineralisation show strong affinities with Fe-Mg skarns (e.g., SD42/126.3, SD42/155 and SD42/156.46).

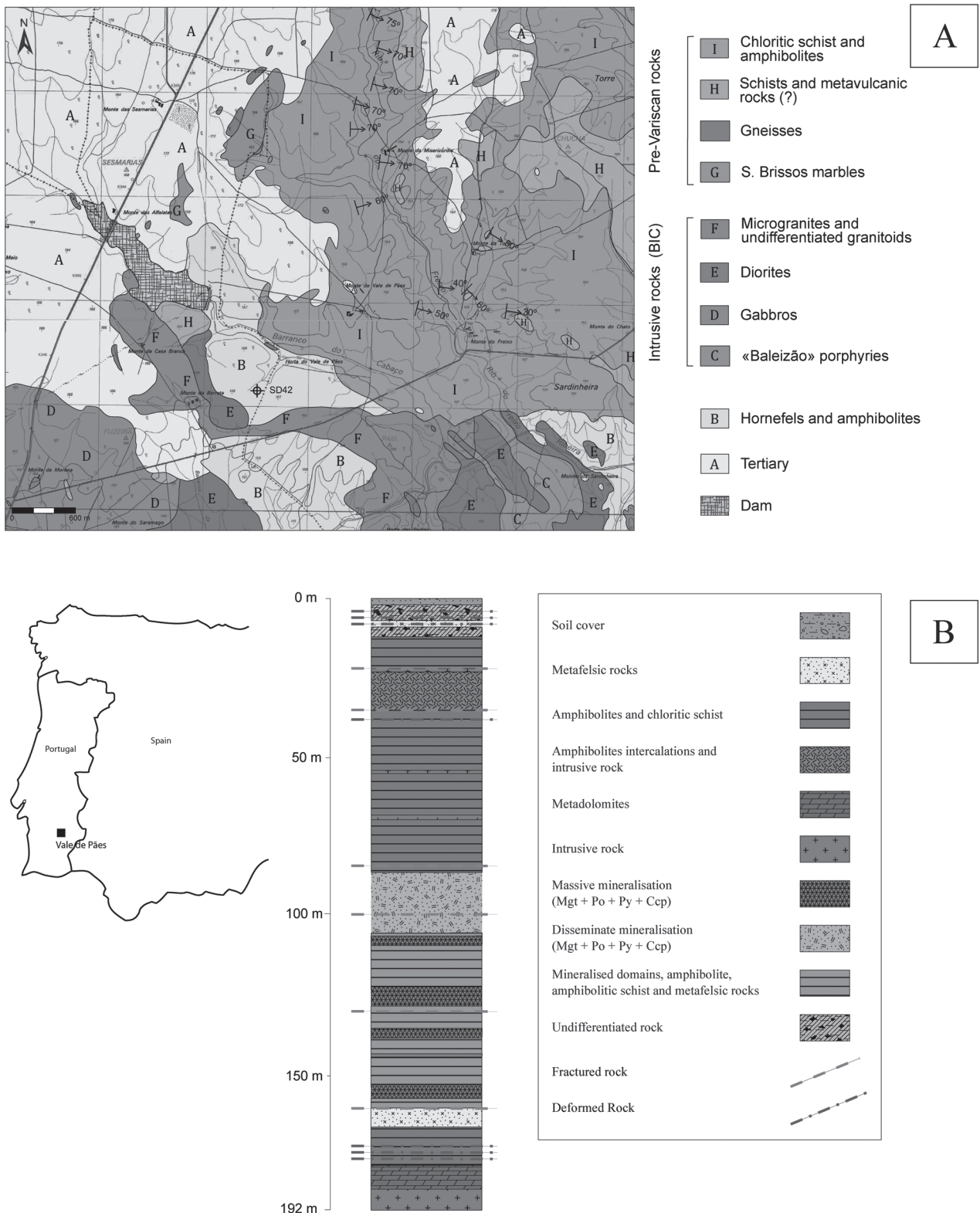


Fig. 1.—A) Geological map of the area surrounding the Vale de Pães deposit (adapted from Serviço de Fomento Mineiro, 1980 *approx.*) and B) schematic representation of the SD42 drill-hole core log (adapted from Serviço de Fomento Mineiro, 1968).

Table 1.—Representative analysis of pyroxene and olivine in the Vale de Pães mineralised domains and respective cation distribution per formula unit. Elemental compositions obtained with JEOL JCSA 733-CG electronic microprobe

Pyroxene	SD42/95					Olivine	SD42/155 (n = 4)	SD42/156.46 (n = 3)
	SD42/92 (n = 3)	Border 168	Border 170	SD42/126.30 (n = 3)	SD42/155 (n = 3)			
<i>Oxides (wt.%)</i>						<i>Oxides (wt.%)</i>		
SiO ₂	53.02	50.09	52.97	54.60	54.36	SiO ₂	37.11	37.28
TiO ₂	0.01	0.13	0.04	0.00	0.02	TiO ₂	0.01	0.02
Al ₂ O ₃	0.58	1.38	0.70	0.59	1.20	Al ₂ O ₃	0.00	0.00
Cr ₂ O ₃	0.00	0.04	0.02	0.02	0.00	Cr ₂ O ₃	0.00	0.00
MgO	14.88	6.53	12.89	15.83	15.36	MgO	33.34	33.52
CaO	25.42	24.13	25.02	25.35	24.98	CaO	0.01	0.03
MnO	0.18	0.69	0.55	0.12	0.12	MnO	0.84	0.77
FeO	6.01	17.43	7.02	3.25	3.80	FeO	28.82	28.44
NiO	0.00	0.00	0.00	0.00	0.01	NiO	0.00	0.01
Na ₂ O	0.13	0.07	0.24	0.02	0.01	Na ₂ O	0.00	0.00
K ₂ O	0.01	0.00	0.02	0.02	0.00	K ₂ O	0.00	0.00
Total	100.22	100.50	99.44	99.80	99.86	Total	100.13	100.04
<i>Based on 6 oxygen's</i>						<i>Based on 4 oxigen's</i>		
Si	1.95	1.95	1.99	2.00	2.00	SiO ₂	1.53	1.54
Ti	0.00	0.00	0.00	0.00	0.00	FeO	0.99	0.98
Al	0.03	0.06	0.03	0.03	0.05	MnO	0.03	0.03
Cr	0.00	0.00	0.00	0.00	0.00	MgO	2.05	2.06
Mg	0.82	0.38	0.72	0.87	0.84	Total	3.07	3.07
Ca	1.00	1.01	1.00	1.00	0.98			
Mn	0.01	0.02	0.02	0.00	0.00	% Forsterite	67	67
Fe	0.19	0.57	0.22	0.10	0.12	% Fayalite	33	33
Ni	0.00	0.00	0.00	0.00	0.00			
Na	0.01	0.01	0.02	0.00	0.00			
K	0.00	0.00	0.00	0.00	0.00			
% Diopside	81	39	75	89	87			
% Hedenbergite	18	59	23	10	12			
% Johannsenite	1	2	2	0	0			

Petrography, mineralogy and relative chronology of deposition

The Fe-Mg skarn matrix is mostly composed of forsterite (*For*₆₇) and diopside (*Di*₉₀) arranged in a coarse-grained granoblastic texture (Fig. 2A, B and Table 1). These minerals, tracing the prograde stage of skarn development (Fig. 3), are surrounded by *Mgt I* (predominant) and pyrrhotite (*Po I*). *Mgt I* forms massive but heterogeneously fractured aggregates that include (sub)euhedral grains usually displaying spinel (*Spl*) exsolutions; its deposition took place during the final steps of the prograde stage. The shallower mineralised domains are characterised by the predominance of massive *Mgt* showing lesser fracturing, as well as minor re-crystallisation. *Po I* occurs as massive, irregular, variably fractured aggre-

gates, developing complex inter-granular relations with *Mgt I* that suggest close periods of deposition or reflect imbalance/balance conditions established during *Mgt I* re-crystallisation (in the retrograding stage). *Po I* deposition precedes the development of hydrous phyllosilicates belonging to the serpentine group (*Serp*), as well as a fracturing event (affecting this sulphide and *Mgt I*), possibly related to the volume increase in consequence of serpentinisation. Pyrite (*Py I*) forms, usually, idiomorphic grains and develops textural relationships with other mineral phases of dubious interpretation; nonetheless, it appears to be related to the local early change of *Po I*, further recorded by *Py II* + *Mgt II* exsolutions and, sometimes, marcasite (*Mrc*). Chalcopyrite (*Ccp I*) aggregates present very fine granularity and form exsolutions in other sulphides or late replace-

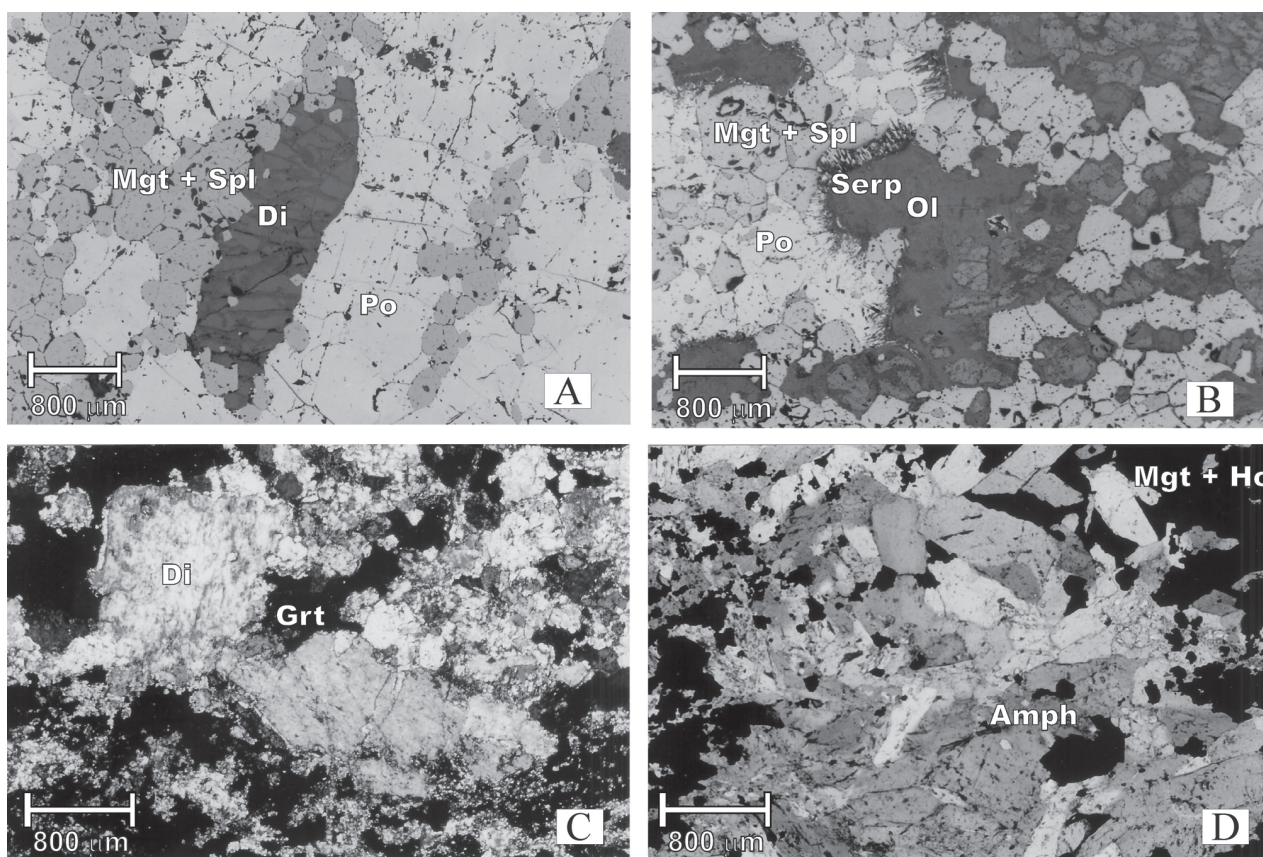


Fig. 2.—Photomicrographs illustrating features of the Vale de Pães mineralisation, A and B) Fe-Mg skarn, C and D) Fe-Ca skarn. A) *Di* surrounded by *Mgt* (re-crystallised, containing *Spl* exsolutions) and *Po*; B) serpentinitised *Ol* encircled by re-crystallised *Mgt*. C) subhedral grain of *Di* and relics of *Grt* partly replaced by late silicates; D) anhedral grains of *Mgt* coexisting with late *Amph* and, sometimes, replacing these silicates. *Di*: diopside; *Mgt*: magnetite; *Spl*: spinel; *Hc*: Hercynite; *Po*: Pyrrhotite; *Grt*: garnet; *Amph*: amphibole; *Ol*: olivine; *Serp*: serpentine.

ments. A carbonatisation event experienced by the Fe-Mg skarn took place after *Mgt I* re-crystallisation, leading to carbonate deposition in veins or differential replacement of the matrix-forming minerals before development of the second generation of sulphides (*Py II* and *Po II*). Hydration processes, such as serpentinisation, are synchronous or run shortly after carbonatisation, and play an important role on the heterogeneous replacement of pyroxene and olivine relics; amphibole (*Amph*) and phlogopite (?), although rare, complete the mineral paragenesis developed during the retrograde stage. The chart in Fig. 3 summarises the paragenetic information concerning the Fe-Mg skarn.

The Fe-Ca skarn matrix is composed of pyroxene and garnet relics (widely replaced by late silicates; Fig. 2C, D) that preserve compositions ranging from diopside (Di_{81}), salite (Di_{75}) and ferrosalite (Di_{39}) (Table 1) and grossularite ($Grs_{86}Alm_{12}$). The late mineral assemblages include mg-hastingsite/par-

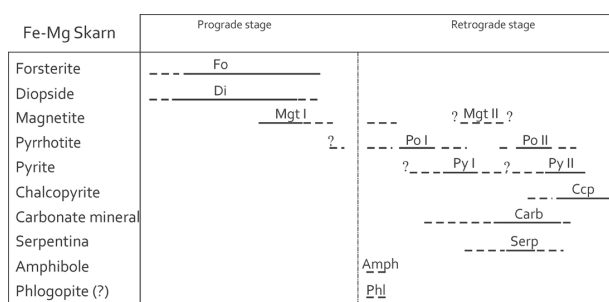


Fig. 3.—Synthesis of the paragenetic information concerning the Vale de Pães Fe-Mg skarn.

gasite, epidote and prehnite, besides rare chlorite, biotite and sphene (Fig. 4). *Mgt I* is the predominant mineral phase in the irregular and massive ore aggregates; this oxide shows hercynite (*Hc*) exsolutions and occurs preferentially associated with amphibole and clinopyroxene grains; in places *Mgt* replaces these silicates, reflecting a long-lived peri-

Fe-Ca Skarn	Prograde stage		Retrograde stage	
Grossular	Grs			
Pyroxene	Px			
Magnetite			Mgt I	Mgt II
Pyrrhotite			Po	
Pyrite			? Py	
Chalcopyrite			Ccp	
Epidote			Ep	
Prehnite			? Prh	
Amphibole		Amph		
Biotite			Bt	
Sphene			? Sph	
Quartz				Qtz

Fig. 4.—Paragenetic information on Vale de Pães Fe-Ca skarn. * Pyroxene composition ranges from diopside to salite/ferrosalite; ** Amphibole composition varies between mg-hastingsite and pargasite.

od of deposition (after deposition of these silicates). Sulphides (*Po*, *Py* and *Ccp*) are scarce and form thin disseminations in matrix. As in the Fe-Mg skarn, the relative chronology of *Py* deposition is hard to determine, but its relation to *Po* alteration/replacement is fairly well documented; occasionally, *Mrc* occurs in equivalent textural context. *Ccp* is very rare and always postdates the remaining sulphides, forming thin exsolutions and replacement rims. Prehnite is a rather late phase, developing aggregates that fill interstitial open spaces. The chart in fig. 4 summarises the paragenetic information available for the Fe-Ca skarn.

Ore geochemistry

Table 2 presents the analytical results available for key samples. In general and comparatively, Fe-Ca skarn samples show, as expected, higher contents of SiO_2 , CaO , Al_2O_3 , Na_2O , MnO , TiO_2 , La, Ce, Nd and Cr than those of Fe-Mg skarn; the latter is characterised by higher values of FeO (t), MgO, S, Cd, Cu, Zn, Co and Ni. The C1 chondrite (Boyn-ton, 1984) normalised patterns of rare-earth elements (REE), although sub-parallel (Fig. 5A), show different fractionation: $\Sigma\text{REE} = 90.64$ and $(\text{La}/\text{Yb})_{\text{cn}} = 5.84$ for SD42/95 sample; $\Sigma\text{REE} = [15.48, 29.21]$ and $(\text{La}/\text{Yb})_{\text{cn}} = [4.31, 4.93]$ for the remaining specimens analysed. In sample SD42/95, the Eu normalised value defines a negative anomaly $(\text{Eu}/\text{Sm})_{\text{cn}} = 0.6$ and possibly the same applies to the remaining samples for which the Eu content is below the detection limit of the analytical method used. According to Wilde *et al.* (1996), anomalies in Ce can be put in evidence through the expression: \log

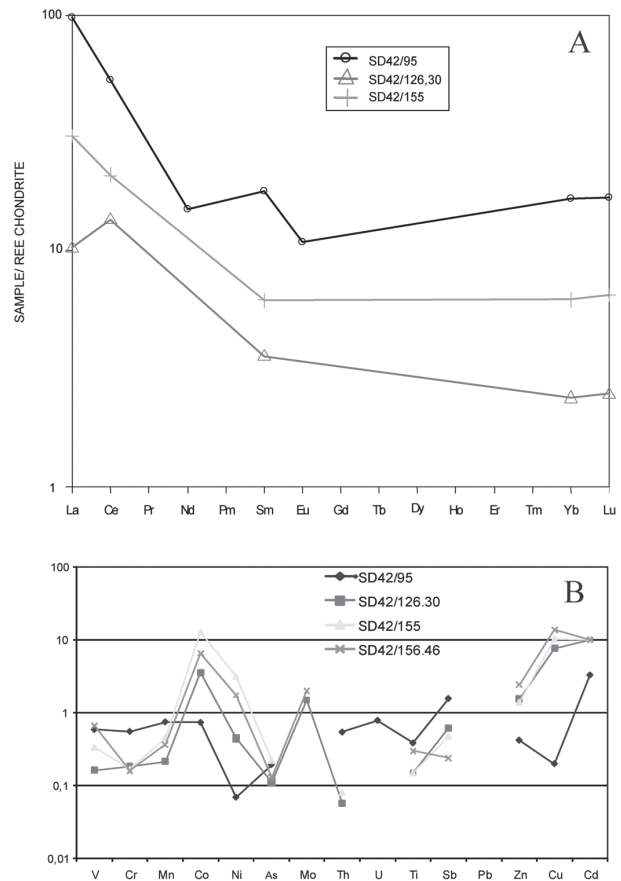


Fig. 5.—A) C1 chondrite (Boyn-ton, 1984) normalised REE patterns. B) RSE and other reference elements normalized patterns (see text for information about the standards used). Samples of the Vale de Pães Fe-Ca (SD42/95) and Fe-Mg skarns (SD42/126.30, SD42/155 and SD42/156.46). Concentrations below the detection limit of the analytical method used were not considered.

$[\text{5Ce}^*/(4\text{La}^* + \text{Sm}^*)]$, where * refers to C1 chondrite normalised contents (Boyn-ton, 1984); on this basis, Ce negative anomalies characterise samples SD42/95 and SD42/155 (-0.19 and -0.08 , respectively), while a positive Ce anomaly stands up for sample SD42/126.3 (0.18).

Contents of some redox sensitive elements (RSE), such as Cr, Mn, Co, Ni, As, Sb, Th and U, were normalised to the *North American Shale Composite* (NASC, Gromet *et al.*, 1984); V values were normalised to the *Marine Shale of Ruhr* (Degens *et al.*, 1958) and those of Mo to the *Recent Sediments* (Wedepohl, 1974). Other reference elements, such as Ti, Pb, Zn, Cu and Cd, were included in this approach, normalising their contents relatively to NASC (Ti) and to *Standard Shales* (Turekian & Wedepohl, 1961). Plots of the normalised RSE con-

Table 2.—Whole-rock analysis of key samples of Vale de Pães Fe-Mg and Fe-Ca skarns

	Method	Fe-Ca skarn		Fe-Mg skarn	
		SD42/95	SD42/126.30*	SD42/155	SD42/156.46*
SiO ₂	RXF	43.14	5.6	14.32	14
Al ₂ O ₃	RXF	11.46	tr.	1.41	tr.
Fe Total (oxides)	RXF	13.83	17.5	61.97	73
MnO	RXF	0.47	0.25	0.33	0.16
CaO	RXF	25.45	0.01	1.97	5
MgO	RXF	3.83	6	11.19	6
Na ₂ O	RXF	0.22	tr.	0.13	tr.
K ₂ O	RXF	< 0.03	tr.	0.04	0.04
TiO ₂	RXF	0.31	0.16	0.12	0.12
P ₂ O ₅	RXF	0.06	tr.	< 0.03	0.03
LOI		1		3.14	
Total		99.77	29.52	94.62	98.35
S%			4.93	8.46	4.17
S%	RXF	0.03			0.05
Ba	RXF	< 3	< 3	< 3	< 3
Rb	RXF	< 3	< 3	< 3	< 3
Sr	RXF	148	15	8	9
Cs	INAA	< 1	< 1	< 1	2
Ta	INAA	< 0.5	< 0.5	< 0.5	< 0.5
Nb	RXF	10	20	20	21
Hf	INAA	2	< 1	< 1	< 1
Zr	RXF	80	28	16	12
Y	RXF	21	< 3	7	< 3
Th	INAA	6.7	0.7	1	< 0.2
U	INAA	2.1	< 0.5	< 0.5	< 0.5
Cr	INAA	69	23	21	20
Ni	ICP	3.88	25.72	183.50	101.00
Co	INAA	19.00	92.00	327.00	169.00
Sc	INAA	12.40	2.30	3.20	1.30
V	ICP	57.60	15.84	33.29	64.78
Cu	ICP	8.96	345.03	468.18	618.40
Pb	ICP	< 3	< 3	< 3	< 3
Zn	ICP	40.03	146.79	133.02	230.60
Bi	ICP	< 2	3.22	< 2	< 2
Cd	DCP	1.00	3.00	3.00	3.00
Sn	RXF	< 4	< 4	< 4	< 4
W	INAA	2.00	< 1	< 1	< 1
Mo	ICP	< 1	2.84	< 1	3.60
Br	INAA	< 0.5	< 0.5	< 0.5	< 0.5
B	DCP	26.00	< 10	< 10	< 10
Be	ICP	1.07	< 1	< 1	< 1
Ag	ICP	< 0.3	0.56	0.45	0.48
Ir (ppb)	INAA	< 5	< 5	< 5	< 5
Au (ppb)	INAA	< 2	< 2	9.00	< 2
Au (ppb)	AA	45.00	59.00	16.00	10.00
Hg	INAA	< 1	< 1	< 1	< 1
As	INAA	5.50	3.20	6.30	3.70
Se	INAA	< 3	< 3	5.00	< 3
Sb	INAA	3.30	1.30	1.00	0.50
La	INAA	30.30	3.20	9.50	< 0.5
Ce	INAA	43.00	11.00	17.00	< 3
Nd	INAA	9.00	< 5	< 5	< 5
Sm	INAA	3.50	0.70	1.20	< 0.1
Eu	INAA	0.80	< 0.2	< 0.2	< 0.2
Tb	INAA	< 0.5	< 0.5	< 0.5	< 0.5
Yb	INAA	3.50	0.50	1.30	< 0.2
Lu	INAA	0.54	0.08	0.21	< 0.05

Concentrations in wt% (oxides of major elements) and ppm (minor elements, except when indicated).

* Semi-quantitative analyses of major element oxides.

tents (Fig. 5B) show sub-parallel patterns for samples representing the Fe-Mg skarn (SD42/155 and SD42/156.46), which differ from the one concerning the Fe-Ca skarn (SD42/95). Note that RSE contents in the latter sample are almost always below the respective standard, highlighting only positive anomalies in Sb and Cd, in addition to a clear depletion in Ni and Cu values. In contrast, the RSE normalised patterns for samples of Fe-Mg skarn show pronounced positive anomalies for Co, Mo, Ni, Zn, Cu, and Cd, denoting significant enrichment relatively to the standard used; the Th and As contents are very low, showing well-marked negative anomalies. The contents of Mn are negligible in all samples of the mineralised domains.

Discussion

Considering the matrix-forming minerals present in mineralised domains, critical information can be inferred by considering the oxidation state reflected by mineral paragenesis developed in the prograde stage (Einaudi *et al.*, 1981, Einaudi & Burt, 1982). Indeed, according to Newberry (1983), the compositions displayed by the grossularite relics in the Vale de Pães Fe-Ca skarn (SD42/95) correspond to those generated in equilibrium with reducing fluids. Additionally, the analysed pyroxenes show significant oscillation in hedenbergitic contents, besides their tendency to increase in the Fe-Ca skarn domains; in the latter, Di_{39} compositions are known in sample SD42/95, suggesting further media reduction (e.g., Einaudi *et al.*, 1981). The mineral paragenesis tracing the final step of the prograde stage experienced by the Fe-Mg skarn ($Fo + Di_{90} + Mgt$), suggests that the upper limit of $a(O_2)$ was closer to that ruled by the Mgt/Hem buffer. In transition to the retrograde stage, redox media conditions and Fe availability allowed the precipitation of sulphides ($Po I$ and $Py I$?, which persisted after the carbonisation process), favouring the development of $Mgt-Hc$ exolutions as well. The redox conditions at this stage were also enough to cause the instability of olivine, leading to the generation of phyllosilicates (serpentine group) and $Mgt II$. The presence of Fe oxides in late veins indicates that $a(O_2)$ conditions near the buffer Hem/Mgt were achieved during the final steps of the retrograde stage.

The distribution of RSE contents testifies enrichments in Cu, Cd, Zn, Co, Ni and Mo (Fig. 5B), consistent with an increase of sulphides (particularly

abundant in the Fe-Mg skarn), also agreeing with the prevalence of reducing conditions during the retrograde stage.

The incipient Mn enrichment (a minor component in Mgt and SpI) is interpreted as reflecting the limited availability of this metal, determined by the original concentration in protolith and/or influenced by its solubility in metasomatic fluids. In fact, the differential mobility of chemical elements is a determinant factor for chemical zoning of many mineralising systems (including those of skarn type) and, in the case of Mn, the enrichment trend is focused on domains far from the source magma (Meinert, 1992, 1997). According to the available data, Mn contents are higher in Fe-Ca skarn intervals [incorporated in pyroxenes (Table 1) and in Mgt , Salgueiro, *in prep.*], hence suggesting the possibility of a position further away from the magmatic source compared to the Fe-Mg skarn position; this inference must be, however, unequivocally demonstrated with comprehensive analytical studies.

Pyroxenes in the Vale de Pães Fe-Mg skarn are mainly diopsidic (Di_{90}) and show Al_2O_3 contents (average $\approx 1:00$ wt%) similar to specimens that are typical of magmatic skarns according to Zharikov (1970). However, the fayalitic component of the olivine included in the (anhydrous) prograde mineral paragenesis (Fa_{33}) is significantly above the values reported by Zharikov (1970) for olivines in those magmatic skarns (*i.e.*, Fa_{5-15}). These data, taken together with the period of Mgt precipitation, can be interpreted as a consequence of the compositional characteristics of the magmatic component involved in the prograde stage, which is consistent with the possibility of placing the Fe-Mg skarn near the magma source. Based on experimental data for the $Fo + Di + Spl$ equilibrium (e.g., Aleksandrov, 1998), early stages of the Fe-Mg skarn development must have occurred at temperatures ≈ 600 °C. This inference is compatible with temperature values calculated for plagioclase (with evidence of re-crystallisation) - edenite (late) pairs included in host rocks (≤ 600 °C) (Salgueiro, *in prep.*), tracing, quite possibly, the heat peak related to the emplacement/cooling of the magmatic intrusion that triggered the development of the ore-forming system.

The Fe-Mg skarn shows ΣREE low values, which can be interpreted as an inherited geochemical characteristic from the protolith subsequently replaced, although the hydrothermal mobility of REE may contribute, at least partly, to explain those totals and some of the features of their normalised concentra-

tion patterns. Indeed, the relative impoverishment of LREE in the Fe-Mg skarn may be related to the circulation of aqueous-carbonic fluids in reducing conditions like those typically involved in carbonatisation processes. Likewise, the positive Ce anomaly in sample SD42/126.30 (Fe-Mg skarn) may reflect anoxic conditions, mainly achieved during the deposition of sulphides (quite significant in this sample) in the course of the retrograde stage. Finally, the negative Eu anomalies (Fig. 5B) are indicative of significant interaction with moderately oxygenated hydrothermal fluids (e.g., Michard & Albarède, 1986).

Following closely the approach proposed by Einaudi *et al.* (1981) and considering $XCO_2 \leq 0.1$, the precipitation of carbonates should have occurred at temperatures below 550 °C, which is compatible with the fact that carbonatisation took place after *Mgt I* re-crystallisation. Olivine hydration (serpentinisation) in the Fe-Mg skarn should trace a new stage in the evolution of the system, being almost synchronous to the carbonate deposition; despite the serpentine mineral group analysed (Salgueiro, *in prep*) do not present ideal stoichiometry due to subsequent changes, their deposition must have occurred at temperatures below 420 °C, as reported by Greenwood (1967b, *in* Einaudi *et al.*, 1981) for similar situations characterised by low partial pressure of volatile and $XCO_2 < 0.05$. Equivalent temperature (less than ≈ 420 °C) conditions can be deduced for the deposition of *Py II*, *Po II* and *Ccp* taking into account their position on the paragenetic sequence. The development of *Po II* and *Py II* crypto-crystalline aggregates is interpreted as evidence of abrupt temperature drop following the relative media reduction, pH decrease and $a(S_2)$ increase.

The formation of prehnite in Fe-Ca skarn suggests that the late stages of hydration took place under conditions of low fluid pressure, which, according to the approach outlined by Einaudi *et al.* (1981) for similar conditions, should have occurred at temperatures below 400 °C. In this context, the scarcity of *Mrc* as a result of *Po* destabilisation, suggests that the decrease in pH during the retrograde stage (also found in iron-magnesian skarn) was not enough to favour the development of this sulphide. Additionally, the relative rarity of *Ccp* (particularly in the Fe-Ca skarn) indicates relative paucity of Cu in the system since there are no physical-chemical reasons that prevent *Ccp* deposition. Moreover, in this geochemical environment, it is expected that the process had involved mineralising fluids with moderate to

high salinity, which is consistent with the relative enrichment in Na reported by the development of mg-hastingsite/pargasite in the Fe-Ca skarn and amphiboles with significant edenitic component in the host rocks (Salgueiro, *in prep*).

Considering several skarn studies (e.g., Einaudi *et al.*, 1981, Meinert, 1992, 1997, and Pons *et al.*, 2009), the spatially coexistence of two skarn types, as interpreted for the Vale de Pães deposit, may be the result of: 1) an overlapping of iron-calcic skarn on iron-magnesian skarn; 2) heterogeneous fluid/rock ratio due to different protolith features; 3) multiple magmatic source fluids and variable interaction with (different?) host protholith; and 4) differences in progression of equilibrium reactions within the metasomatic front. The geological, mineralogical and geochemical data herein documented for the Vale de Pães deposit, suggest, as a first approach that, with the exception of the first hypothesis, all the others are possible, either plain or modified. However, these hypotheses must be comprehensively examined in detailed studies.

Conclusions

During formation of the prograde Fe-Mg and Fe-Ca skarn mineral parageneses only slight $a(O_2)$ variations took place; these mineral parageneses are generally oxidised, but in Fe-Ca skarn a relatively reduced media can be inferred. The physico-chemical conditions (decrease of pH, temperature and increase in the $a(S_2)$) achieved during the retrogradation stage were crucial for sulphide deposition in the Fe-Mg skarn, influencing also the observed chemical zonation. In particular, the circulation of aqueous-carbonic fluids during the late carbonatisation event experienced by the Fe-Mg skarn must have influenced REE mobilization.

Some relevant features (such as the whole-rock Mn and Al contents, and Fa component of olivine), together with the period of *Mgt* precipitation, suggest that the Fe-Mg skarn is positioned relatively close to the magma source.

References

- Aleksandrov, S.M. (1998). *Geochemistry of Skarn and Ore Formation in Dolomites*. VSP, Utrecht, Tokyo, 300 pp.
- Boynton, W.V. (1984). Geochemistry of the rare earth elements: meteorite studies. *In: Rare earth element*

- geochemistry* (Henderson, P., ed.). Elsevier, Amsterdam, 63-114.
- Carvalho, D. (1976). Les gisements de fer du Portugal. *In: The iron ore deposits of Europe and adjacent areas* (Zitzmann, A., ed.), Commission for the Geological Map of the World, Subcommission for the Metallogenic Map of the World, Hannover, 255-260.
- Carvalho, D. & Oliveira, V. (1992). Recursos minerais. *In: Notícia Explicativa da Folha 8: Carta Geológica de Portugal na escala 1:200 000*. Serviços Geológicos de Portugal, 81-83.
- Degens, E.T.; Williams, E.G. & Keith, E.G. (1958). Application of geochemical criteria [Pennsylvania], part 2 of environmental studies of carboniferous sediments. *American Association of Petroleum Geologists Bulletin*, 42: 981-997.
- Einaudi, M.T. & Burt, D.M. (1982). Introduction - terminology, classification, and composition of skarn deposits. *Economic Geology*, 77: 745-754. doi:10.2113/gsecongeo.77.4.745
- Einaudi, M.T.; Meinert, L.D. & Newberry, R.J. (1981). Skarn deposits. *Economic Geology, 75th Anniversary Volume*: 317-391.
- Gromet L.P.; Dymek, R.F.; Haskin L.A. & Korotev, R.L. (1984). The "North American shale composite": its compilation, major and trace element characteristics. *Geochimica et Cosmochimica Acta*, 48: 2469-2482. doi:10.1016/0016-7037(84)90298-9
- Meinert, L.D. (1992). Skarns and skarn deposits. *Geoscience Canada*, 10: 145-162.
- Meinert, L.D. (1997). Application of skarn deposit zonation models to mineral exploration. *Exploration and Mining Geology*, 6: 185-208.
- Michard, A. & Albarède, F. (1986). The REE content of some hydrothermal fluids. *Chemical Geology*, 55: 51-60. doi:10.1016/0009-2541(86)90127-0
- Oliveira, V. (1986). Prospecção de minérios metálicos a sul do Tejo. *Geociências - Revista da Universidade de Aveiro*, 1: 15-22.
- Piçarra, J.; Oliveira, V. & Oliveira, T. (1992). Paleozóico. *In: Notícia Explicativa da Folha 8, Carta Geológica de Portugal, escala 1:200000*, Lisboa, Serviços Geológicos de Portugal, 25-30.
- Pons, J.M.; Franchini, M.; Meinert, L.; Recio, C. & Etcheverry, R. (2009). Iron Skarns of the Vegas Peladas District, Mendoza, Argentina. *Economic Geology*, 104: 157-184.
- Purtov, V.K.; Kholodnov, V.V.; Afilogov, V.N. & Nechkin, G.S. (1989). The role of chlorine in the formation of magnetite skarns. *International Geology Review*, 31: 63-71. doi:10.1080/00206818909465861
- Salgueiro, R.M.M. (*in prep.*). *Caracterização e génese das mineralizações de magnetite - sulfuretos de Monges (Santiago do Escoural, Montemor-o-Novo) e ensaio comparativo com as suas congêneres em Orada e Vale de Pães (Serpa - Vidigueira)*. Tese de Doutoramento (PhD Thesis), Universidade de Lisboa, Lisboa.
- Serviço de Fomento Mineiro (1968). *Descrição da sondagem, n.º 42 de Vale de Pães*. Serviço de Fomento Mineiro, Relatório Interno, Beja.
- Serviço de Fomento Mineiro, 1980 (*aprox.*), *Cartas Geológicas na escala 1:25000, n.º 499 (Cuba) e n.º 510 (S. Matias)*. Serviço de Fomento Mineiro, Beja.
- Turekian, K.K. & Wedepohl, K.H. (1961). Distribution of the elements in some major units of Earth's crust. *Geological Society of American Bulletin*, 72: 175-192. doi:10.1130/0016-7606(1961)72[175:DOTEIS]2.0.CO;2
- Wedepohl, K.H. (1974). *Handbook of Geochemistry*. Springer-Verlag, Berlin, 374 pp.
- Wilde, P.; Quinby-Hunt, M.S. & Erdtmann, B.D. (1996). The whole-rock cerium anomaly: a potential indicator of eustatic sea-level changes in shales of the potential indicator of eustatic sea-level changes in shales of anoxic facies. *Sedimentary Geology*, 101: 43-53. doi:10.1016/00370738(95)00020-8
- Zharikov, V.A. (1970). Skarns. *International Geology Review*, 12: 541-559, 619-647, 760-775. doi:10.1080/00206817009475262

Recibido el 3 de diciembre de 2009
 Aceptado el 18 de marzo de 2010
 Publicado online el 19 de mayo de 2010